Catalytic control of enzymatic fluorine specificity

Amy M. Weeks[a] and Michelle C. Y. Chang[a,b,c,1]

Departments of [a]Chemistry and [b]Molecular and Cell Biology, University of California, Berkeley, CA 94720; and [c]Physical Biosciences Division, Lawrence Berkeley National Laboratory, Berkeley, CA 94720

Edited by Perry Allen Frey, University of Wisconsin-Madison, Madison, WI, and approved October 24, 2012 (received for review July 21, 2012)

The investigation of unique chemical phenotypes has led to the discovery of enzymes with interesting behaviors that allow us to explore unusual function. The organofluorine-producing microbe *Streptomyces cattleya* has evolved a fluoroacetyl-CoA thioesterase (FlK) that demonstrates a surprisingly high level of discrimination for a single fluorine substituent on its substrate compared with the cellularly abundant hydrogen analog, acetyl-CoA. In this report, we show that the high selectivity of FlK is achieved through catalysis rather than molecular recognition, where deprotonation at the C_α position to form a putative ketene intermediate only occurs on the fluorinated substrate, thereby accelerating the rate of hydrolysis 10^4-fold compared with the nonfluorinated congener. These studies provide insight into mechanisms of catalytic selectivity in a native system where the existence of two reaction pathways determines substrate rather than product selection.

enzyme mechanism | substrate selectivity

Living organisms have solved some of the most difficult challenges in catalysis by harnessing the exquisite selectivity and reactivity of enzyme active sites to build complex chemical behaviors (1–5). Indeed, the plasticity of enzymes toward evolution of new function has allowed life to flourish in diverse biospheres by conferring a selective advantage to hosts that can demonstrate catalytic innovation and use unusual resources. The enzymes that form the molecular basis for these chemical phenotypes are a rich source of molecular diversity and provide an experimental platform for the continual search to gain insight into the mechanisms and dynamics of protein and organismal evolution (6–9). One of the salient features of enzymes is their extremely high substrate selectivity, which allows them to choose the correct substrate over the thousands of other small molecules that are present in cells at any given time. Thus, the exploration of substrate specificity and its evolution is key for understanding both enzyme catalysis and the expansion of biodiversity at the molecular level (7–12).

In this context, a singular chemical trait found in the soil bacterium *Streptomyces cattleya* is its ability to catalyze the formation of carbon–fluorine bonds (13, 14). Fluorine resides at one corner of the periodic table, and its unique elemental properties make it highly effective as a design element for drug discovery but also quite challenging for the synthesis of fluorine-containing molecules (15–17). Although fluorine has emerged as a common motif in synthetic compounds, including top-selling drugs such as atorvastatin and fluticasone, it has been underexploited in nature, and only a few biogenic organofluorine compounds (<20) have been identified to date despite the thousands of known natural products containing chlorine and bromine (~5,000) (18, 19). In fact, the only fully characterized organofluorine natural products are derived from a single pathway that produces the deceptively simple poison fluoroacetate (**1**). The high toxicity of fluoroacetate arises from its antimetabolite mode of action resulting from the substitution of one hydrogen in acetate (**2**), an important cellular building block, with fluorine. As a consequence of this conservative structural change, fluoroacetate can still enter normal acetate metabolism via activation to fluoroacetyl-CoA (**3**) but then acts as a mechanism-based inhibitor of the tricarboxylic acid (TCA) cycle upon conversion to fluorocitrate (**4**) and elimination of fluoride at a critical point (20, 21) (Fig. 1*A*).

The potency of fluoroacetate as a poison poses an especially difficult substrate selectivity problem at the cellular level for the host organism, where a single fluorine atom must be recognized very specifically over hydrogen to clear very low endogenous levels of toxic fluoroacetyl-CoA while simultaneously maintaining the high levels of acetyl-CoA (**5**) required for cell growth and survival. Consequently, there exists a natural selective pressure on *S. cattleya* to meet this challenge, and it has evolved a fluoroacetyl-CoA thioesterase (FlK) that catalyzes the breakdown of fluoroacetyl-CoA to prevent lethal synthesis of fluorocitrate (Fig. 1*A*) (22–24). We have recently shown that FlK demonstrates an extremely high, 10^6-fold selectivity for hydrolysis of fluoroacetyl-CoA over acetyl-CoA based on a decrease in K_m (10^2) and increase in k_{cat} (10^4) for the fluorinated substrate (24). Although the K_m of FlK with respect to fluoroacetyl-CoA (8 μM) is significantly lower than that for acetyl-CoA (2 mM), it is interesting to note that FlK likely operates near saturation for both substrates in vivo, given the high intracellular concentration of acetyl-CoA (25), with substrate selectivity governed by the rate of hydrolysis (k_{cat}) rather than substrate binding (K_d). We thus set out to explore the molecular origin of the catalytic selectivity of FlK with regard to fluorine and now report the existence of an unexpected C_α-deprotonation pathway for enzymatic thioester hydrolysis, through a putative ketene intermediate, that serves as the basis for fluorine discrimination.

Results

Elucidating the Kinetic Basis for Fluorine Selectivity. The hydrolysis of thioesters typically involves direct attack of the nucleophile at the carbonyl group to form a tetrahedral intermediate, which subsequently collapses to produce the free carboxylic acid and thiol end products. The fluorine substitution itself activates the carbonyl moiety toward nucleophilic attack through inductive effects and provides a potential mechanism for discrimination between fluoroacetyl- and acetyl-CoA (*SI Appendix*, Fig. S1). However, the rate of chemical hydrolysis of fluoroacetyl-CoA at neutral pH is only 10-fold faster compared with acetyl-CoA, rather than 10^4-fold, as occurs in the FlK active site (24). Even at pH >13, the largest difference in reactivity that we observe for chemical hydrolysis is 100-fold (*SI Appendix*, Fig. S2). These observations suggest that the large rate acceleration of FlK with respect to fluoroacetyl-CoA may originate from more than a simple increase in the electrophilicity of the carbonyl group upon fluorine substitution. To further probe the role of carbonyl activation in FlK substrate selectivity, we prepared a set of acyl-CoA analogs (**3**, **5**–**11**) with different functional groups at the α position, thereby accessing a wide range of values of the polar substituent constant (σ^*) that describes the activation of the acyl-CoA carbonyl group toward nucleophilic attack (26). By examining the relationship between σ^* and the rate of reaction, this series of

Author contributions: A.M.W. and M.C.Y.C. designed research; A.M.W. performed research; A.M.W. and M.C.Y.C. analyzed data; and A.M.W. and M.C.Y.C. wrote the paper.

The authors declare no conflict of interest.

This article is a PNAS Direct Submission.

[1]To whom correspondence should be addressed. E-mail: mcchang@berkeley.edu.

This article contains supporting information online at www.pnas.org/lookup/suppl/doi:10.1073/pnas.1212591109/-/DCSupplemental.

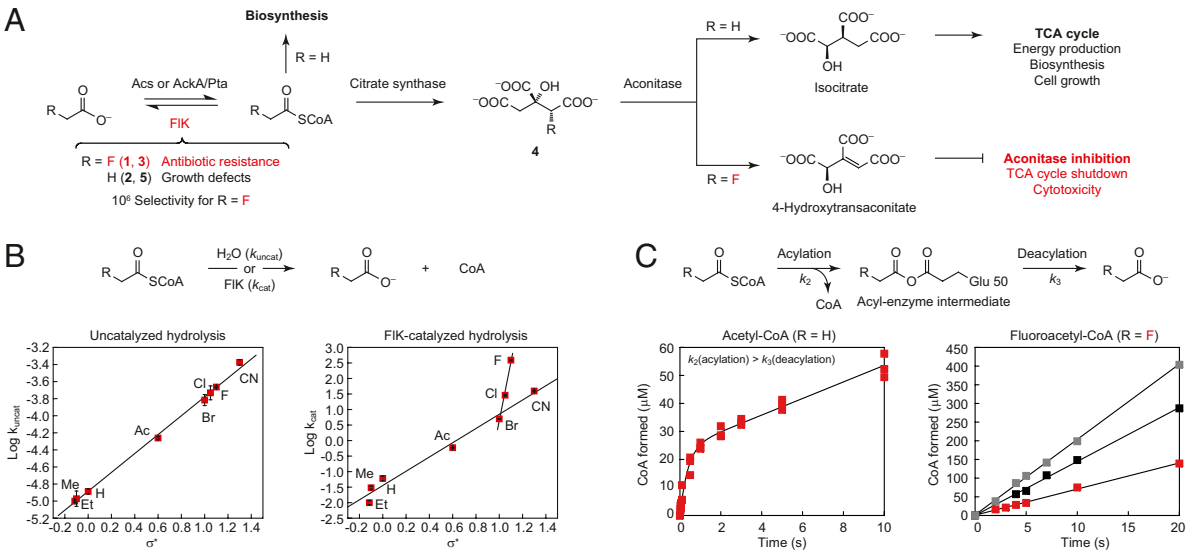

Fig. 1. FlK selectivity for fluoroacetyl-CoA over acetyl-CoA is derived from a change in the rate-limiting step in thioester hydrolysis. (*A*) FlK catalyzes the hydrolysis of fluoroacetyl-CoA, which reverses the lethal synthesis of an irreversible aconitase inhibitor. (*B*) Taft free-energy relationship analysis of uncatalyzed (*Left*) and FlK-catalyzed (*Right*) acyl-CoA hydrolysis. Pseudo-first-order rate constants were determined by linear fitting (for uncatalyzed reactions) or by fitting a plot of initial rate versus substrate concentration to the Michaelis-Menten equation (for FlK-catalyzed reactions). Ac, acetyl; Et, ethyl; Me, methyl. (*C*) Pre-steady-state kinetics of FlK-catalyzed acetyl-CoA (*Left*, 25 μM FlK) and fluoroacetyl-CoA hydrolysis (*Right*; red squares, 25 μM FlK; black squares, 50 μM FlK; grey squares, 75 μM FlK).

compounds can be used to assess the relative contribution of the α substituent toward acyl-CoA hydrolysis.

We found a linear relationship between σ* and the logarithm of the pseudo-first-order rate constant for chemical hydrolysis of the acyl-CoAs at neutral pH, implying that they share a common mechanism and transition state for the overall transformation under these conditions (Fig. 1*B* and *SI Appendix*, *Discussion*). In comparison, the same plot for FlK-catalyzed acyl-CoA hydrolysis produces two intersecting lines, with the chlorinated and fluorinated substrates being hydrolyzed at rates faster than predicted by σ*, suggesting a change in transition-state structure, rate-limiting step, or chemical mechanism for halogenated substrates compared with nonhalogenated substrates (Fig. 1*B* and *SI Appendix*, Fig. S3). An alternative explanation for this difference in behavior is that FlK actually binds a different form of the fluoroacetyl-CoA substrate, which has higher potential to form a hydrate or enolate in aqueous solution compared with other less polarized acyl-CoAs such as acetyl-CoA (*SI Appendix*, Fig. S1). However, NMR studies showed no evidence for formation of a hydrate or enolate of fluoroacetyl-CoA under these conditions within the limit of detection (*SI Appendix*, Fig. S1). From the Taft analysis and these control experiments, it appears that the fluorine-dependent selectivity of FlK could then be related to a change in the rate-determining step or catalytic mechanism of hydrolysis between the two substrates.

We began to explore the basis of this difference in reactivity by comparing the pre-steady-state kinetic behavior of FlK with respect to acetyl-CoA and fluoroacetyl-CoA. With acetyl-CoA, one equivalent of free CoA is formed in a burst phase (k_2) during the first turnover before the steady state is reached ($k_3 = k_{cat}$), which indicates that there is a slow step in the catalytic cycle subsequent to CoA formation (Fig. 1*C*). A burst phase can result from rapid chemistry involved in the conversion of substrate to product followed by a rate-determining physical event, such as product release or some other conformational change required for catalysis (27). The steady-state rate constant (k_{cat}) following the burst would then correspond mainly to the rate of this physical event rather than a chemical step in the catalytic mechanism. However, burst phases are also often observed in cases where a conformational change is not rate-limiting and are derived instead from fast formation of an enzyme-bound intermediate before a rate-limiting catalytic step (28). With regard to FlK, hydrolases represent a canonical example of covalent catalysis where the burst phase is derived from rapid enzyme acylation by the substrate followed by slower enzyme deacylation as the rate-determining step (29). Furthermore, recent studies of a 4-hydroxybenzoyl-CoA thioesterase (4-HBT) from the FlK superfamily have shown that CoA is formed in a burst with exchange of protein-derived oxygen into the carboxylic acid, which provides strong support for the formation of an enzyme anhydride on the active-site glutamate of the catalytic triad (30, 31).

To test for the intermediacy of an enzyme–anhydride in FlK-catalyzed hydrolysis of acetyl-CoA, we carried out trapping experiments with hydroxylamine. Nucleophilic attack of hydroxylamine on the putative enzyme anhydride could occur either at the substrate-derived or enzyme-derived carbonyl group to regenerate the native enzyme or convert the carboxylate side chain to a hydroxamate, respectively (*SI Appendix*, Fig. S4). Notably, no covalent modification of the enzyme is expected for hydroxylamine trapping of other types of acyl-enzyme intermediates, such as esters, because the electrophilic carbonyl group in these cases is derived from the substrate and the native enzyme is regenerated upon reaction with nucleophiles. Tandem mass spectrometry analysis of FlK after incubation with an excess of acetyl-CoA followed by rapid quenching with urea in the presence of hydroxylamine revealed a 15-Da modification on E50 corresponding to conversion of the glutamate side chain to a hydroxamate (*SI Appendix*, Fig. S4). In contrast, no modification was detected in a control sample in which FlK was treated with urea and hydroxylamine in the absence of acetyl-CoA (*SI Appendix*, Fig. S4).

Based on these results, we propose that the burst kinetics observed with acetyl-CoA result from the formation of a covalent acyl-enzyme intermediate on E50 concomitant with formation of free CoA (Fig. 1*C*). Although anhydrides are high in energy, these acyl-enzyme intermediates have been previously documented in biological catalysis, including in thioesterases of both the hotdog-fold (30, 31) and crotonase (32) superfamiles. The burst rate for CoA formation (k_2) for FlK then describes the rate of enzyme acylation, which is followed by the rate-limiting step (k_{cat}) in the catalytic cycle (Fig. 1*C*). The dependence of k_{cat} on the electron-withdrawing ability of the α substituent but

lack of correlation with other parameters such as size strongly suggests that the slow step in FlK turnover involves a chemical transformation of the acyl-enzyme intermediate, rather than a rate-determining conformational change (Fig. 1*B*). Although our previous crystallographic studies had suggested a role for opening of the F36 "gate" in product release, mutation of this residue to form a constitutively open enzyme does not affect the rate of hydrolysis of either acetyl-CoA or fluoroacetyl-CoA (24), suggesting that this motion is not rate-limiting. Furthermore, the insensitivity of k_{cat} to addition of a viscogen [30% (wt/vol) sucrose] rules out the contribution of diffusional steps, such as product release, to rate limitation (*SI Appendix*, Fig. S4). We therefore interpret the steady-state rate of hydrolysis of acetyl-CoA ($k_{cat} = k_3$) to represent a chemical step in FlK catalysis related to enzyme deacylation (Fig. 1*C*).

In comparison, FlK shows no evidence of burst kinetics with fluoroacetyl-CoA based on the fact that the linear fits for product formation at different enzyme concentrations all intersect the *y* axis at 0 (Fig. 1*C* and *SI Appendix*, *Discussion*). The sucrose independence of the rate of hydrolysis of fluoroacetyl-CoA (*SI Appendix*, Fig. S4) implies that a chemical step remains rate-limiting and our kinetic data are thus consistent with two mechanisms. One possibility is that fluoroacetyl-CoA hydrolysis does not involve an acyl-enzyme intermediate and therefore has a single kinetic phase. A second possibility is that enzyme acylation is the slow step in the catalytic cycle ($k_{cat} = k_2$) and that the following steps are faster ($k_3 > k_2$). Although we were unable to observe hydroxylamine modification of FlK in trapping experiments in which fluoroacetyl-CoA was used as the substrate, we cannot rule out formation of an acyl-enzyme intermediate at this time. First, the single-phase kinetic behavior with respect to CoA formation suggests that the breakdown of any intermediate would be faster than its formation and prevent its accumulation for reaction with hydroxylamine. Additionally, the electron-withdrawing fluorine substituent may favor reaction of hydroxylamine at the substrate-derived carbonyl, which would mask the formation of an enzyme–anhydride. Although these two mechanistic possibilities cannot be distinguished at this point, the data are all consistent with a model in which fluorine selectivity arises from a change in the chemical mechanism or rate-limiting step of the reaction between acetyl-CoA and fluoroacetyl-CoA.

Identifying the Chemical Mechanism for Fluorine Selectivity in FlK-Catalyzed Thioester Hydrolysis. We next turned our attention to using evolutionary relationships to gain insight into the chemical mechanisms of the different kinetic behaviors observed for each substrate. Interestingly, FlK appears at the sequence and structural levels to be a chimera of two hotdog-fold superfamilies– the 4-HBT thioesterases and the MaoC dehydratases (Fig. 2*A* and *SI Appendix*, *Discussion* and Fig. S5). At a structural level, FlK possesses a distinctive hydrophobic lid (*SI Appendix*, Fig. S5) that is not found in any of the other crystallographically characterized thioesterases but is shared with the dehydratase family (33). Moreover, the lid is functionally important in FlK for molecular recognition of fluorine via a gatekeeper residue (F36) (24), which is conserved among dehydratases even though it is unique compared with FlK's closest orthologs (*SI Appendix*, Fig. S5). However, FlK shares its catalytic dyad/triad (E50, H76, T42) and putative acyl-enzyme intermediate with the 4-HBT thioesterases. Despite its similarities to the 4-HBT thioesterases, the weaker oxyanion hole and key role of H76 in FlK hydrolysis are more reminiscent of the dehydratases, which use an active-site histidine to remove a proton at the α position of 3-hydroxyacyl-CoA substrates (Fig. 2*A*) (33). Thus, we reasoned that FlK might use a dehydratase-like mechanism for hydrolysis initiated by C_α deprotonation of either the fluoroacetyl-CoA substrate or the acyl-enzyme intermediate to discriminate between fluoroacetyl-CoA and acetyl-CoA based on the lowered pK_a of the protons on the fluorine-substituted carbon.

If a dehydratase-like mechanism were operative in direct deprotonation of the fluoroacetyl-CoA substrate, we would expect k_{cat} to be sensitive to deuterium substitution on the α carbon. However, if C_α deprotonation occurred on an acyl-enzyme intermediate instead, the intrinsic kinetic isotope effect (KIE) would be masked by the slower rate of enzyme acylation with the fluorinated substrate. In this scenario, we would only be able to observe an apparent KIE with labeled substrate if deuteration were to slow down C_α deprotonation such that it becomes at least partially rate-limiting. To test for C_α deprotonation, we prepared ^{2}H-labeled acetyl- (**12**) and fluoroacetyl-CoA (**13**) and measured the rates of their hydrolysis by FlK. For [$^2H_3$]acetyl-CoA, deuterium substitution had no impact on the reaction rate (Fig. 2*B*). In contrast, we observed an apparent primary KIE of 2.4 ± 0.1 for hydrolysis of [$^2H_2$]fluoroacetyl-CoA by FlK (Fig. 2*B*). The magnitude of the KIE for fluoroacetyl-CoA hydrolysis is on the order of or larger than KIEs measured for other characterized enzymes that catalyze C_α deprotonation (34, 35). In comparison, enzymes that carry out nucleophilic attack at a carbonyl moiety typically show an inverse isotope effect, if any, with similarly labeled substrates (36). To further confirm the ability of FlK to initiate C_α deprotonation, we assayed the 3,3,3-trifluoropropionyl-CoA (**14**) substrate and

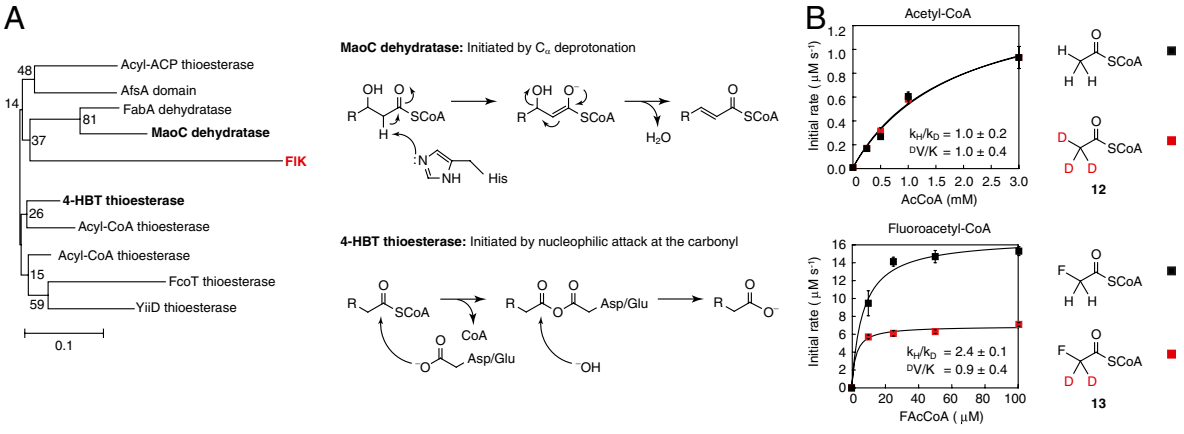

Fig. 2. Breakdown of the fluoroacetyl-enzyme intermediate is accelerated by C_α-deprotonation. (*A*) Structure-based sequence alignment and phylogenetic analysis of the hotdog superfamily indicate that FlK shares functional features with both the 4-HBT thioesterases, which use an enzyme anhydride intermediate in hydrolysis, and the MaoC dehydratases, which initiate dehydration by C_α deprotonation using a catalytic histidine residue. (*B*) Deuteration at the α position of fluoroacetyl-CoA leads to a 2.4-fold kinetic isotope effect (KIE) on k_{cat} for FlK-catalyzed fluoroacetyl-CoA hydrolysis, whereas deuteration at the α position of acetyl-CoA has no impact on the rate constant.

observed rapid formation of one equivalent of CoA followed by elimination of one equivalent of fluoride, suggesting formation of an enolate or carbanion species (37) (*SI Appendix*, Fig. S6). Time-dependent inactivation of the enzyme occurs on the same timescale as CoA formation, which is consistent with stoichiometric enzyme alkylation by the Michael acceptor produced in the active site after loss of fluoride (*SI Appendix*, Fig. S6). Taken together, these data support a model in which substrate selectivity is determined by the existence of a C_α-deprotonation pathway that is only available to activated substrates (Fig. 3*A*).

We further examined the pre-steady-state kinetic behavior of FlK with respect to the [$^2H_2$]fluoroacetyl-CoA substrate and observed a burst phase of CoA formation during the first turnover of the reaction (*SI Appendix*, Fig. S7). The onset of burst kinetics with the deuterated substrate suggests that isotopic substitution slows steps in the catalytic cycle subsequent to the formation of CoA and that C_α deprotonation may occur on an intermediate rather than directly upon the fluoroacetyl-CoA substrate itself. Indeed, the absence of a primary $^D(V/K)$ isotope on fluoroacetyl-CoA hydrolysis, within error, is consistent with a model in which the isotopically sensitive step takes place after the first irreversible step, which would involve formation of free CoA. These behaviors are consistent with the observed KIE and potentially with the existence of a covalent intermediate with the fluorinated substrate. If deprotonation of the fluorinated substrate does occur subsequent to formation of an acyl-enzyme intermediate, then the intrinsic KIE for this step may be larger than the apparent KIE measured with [$^2H_2$]fluoroacetyl-CoA.

Another testable prediction from our model is that if H76 plays a general base role in FlK analogous to that in the dehydratases (Fig. 2*A*), selectivity for fluoroacetyl-CoA over acetyl-CoA should be lost when this residue is mutated because the pathway to C_α deprotonation of the fluorinated substrate would be eliminated. Consequently, both substrates would react via the same mechanism of rate-limiting water attack at the substrate carbonyl, which we would observe experimentally as the disappearance of the KIE for fluoroacetyl-CoA hydrolysis. If an acyl-enzyme intermediate is formed with the fluorinated substrate, we would also expect to see burst kinetics with this mutant. Interestingly, our previous mutagenesis experiments showed that H76 is the most important residue in the catalytic triad and that mutation to alanine resulted in an unexpectedly large kinetic defect compared with other members of the hotdog thioesterase superfamily (24). The H76A mutant was assayed and confirmed to exhibit burst kinetics in the pre-steady-state with both substrates, which implies that an intermediate may also be formed with fluoroacetyl-CoA concomitant with CoA formation (Fig. 3*B*). The insensitivity of k_{cat} to the presence of sucrose suggests again that the observed burst behavior arises from a rate-limiting chemical step rather than a diffusion-controlled physical event (*SI Appendix*, Fig. S8). Strikingly, this mutant demonstrates no selectivity beyond what is expected from polarization for the fluorinated substrate over the non-fluorinated substrate in k_{cat} or in the individual rate constants, k_2 and k_3, indicating that the selectivity for fluorine is directly related to the role of H76. Moreover, the KIE observed with [$^2H_2$]fluoroacetyl-CoA is abolished in the H76A mutant, showing that H76 is directly involved in C_α deprotonation (*SI Appendix*, Fig. S8). Taken together, these experiments highlight the importance of H76 and the C_α-deprotonation pathway in controlling the fluorine specificity of FlK, which is conferred by catalytic selectivity of the enzyme that distinguishes between the two substrates.

Ketene Intermediate in Thioester Hydrolysis. In FlK-catalyzed hydrolysis of the fluorinated thioester, the most likely mechanism that accounts for the observed rapid rate of product formation following proton abstraction is the formation of a fluoroketene intermediate on FlK followed by rapid hydration (Fig. 3*A*). Although unprecedented for enzymatic thioester hydrolysis of a physiological substrate, the utilization of a C_α-deprotonation strategy by FlK is reminiscent of well-characterized chemical model systems with acidic α protons that are known to pass through a ketene intermediate (38, 39). These systems demonstrate a characteristic acceleration in the rate of thioester hydrolysis under conditions where the C_α-deprotonation pathway is accessible, thereby outcompeting the rate of thioester hydrolysis by nucleophilic attack at the carbonyl group at high pH despite the increase in hydroxide concentration (38–40).

An alternative, but less probable, mechanism would require attack of water directly on the enolate or carbanion species (*SI Appendix*, Scheme S1), which is predicted to be slower than direct attack of water on the neutral enzyme-anhydride as observed for acetyl-CoA based on work in chemical model systems (41) (Fig. 3*A*). This alternative mechanism seems unlikely to explain the observed rate acceleration for FlK deacylation because the presence of carbanion character would be expected to deactivate the carbonyl toward nucleophilic attack based on charge repulsion between the approaching nucleophile and the carbanion. Indeed, in chemical model systems involving breakdown of an enolate through a carbanion intermediate, the rate of reaction is one to two orders of magnitude slower than the expected rate of a ketene-based mechanism (41). The formation of a ketene during the FlK catalytic cycle is consistent with the lack of D_2O wash-in at the α

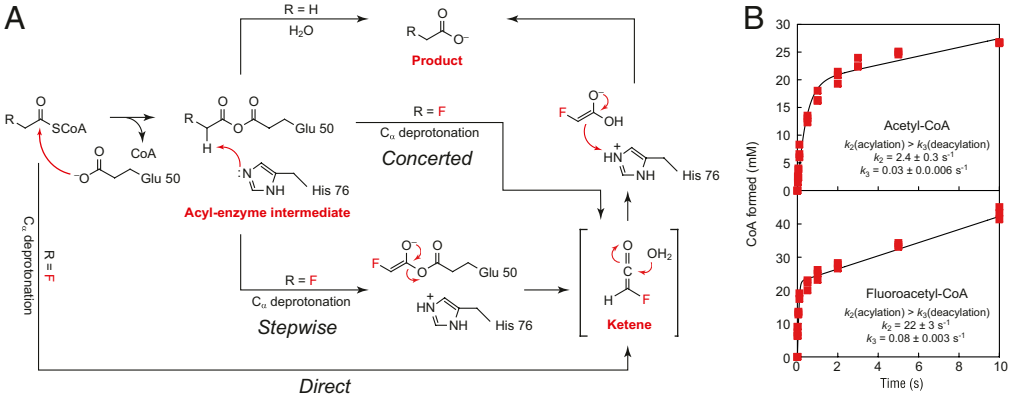

Fig. 3. A change in catalytic mechanism accounts for FlK's specificity for fluoroacetyl-CoA. (*A*) Proposed enzymatic mechanisms for hydrolysis of fluoroacetyl-CoA versus acetyl-CoA. Whereas acetyl-CoA is hydrolyzed through an acyl-enzyme intermediate, fluoroacetyl-CoA could be either directly deprotonated (direct) or deprotonation could occur from a fluoroacetyl-enzyme intermediate in either a stepwise or concerted fashion. (*B*) Pre-steady-state kinetic traces for hydrolysis of acetyl-CoA (*Upper*) and fluoroacetyl-CoA (*Lower*) by FlK-H76A.

position of the fluoroacetate product (*SI Appendix*, Fig. S9), which may imply that hydration takes place more rapidly than proton exchange at H76, as well as with the order of magnitude slower rate of turnover of cyanoacetyl-CoA, which chemical model systems suggest is hydrolyzed via nucleophilic attack on the carbanion species (40, 41).

Discussion

Streptomyces cattleya is faced with an unusually difficult problem in substrate selectivity, where a single fluorine substituent must be recognized over hydrogen to detoxify low levels of endogenous fluoroacetyl-CoA while maintaining high concentrations of the cellular acetyl-CoA pool. The level of discrimination displayed by FlK is surprisingly high given the promiscuity of the other characterized members of the hotdog-fold thioesterase superfamily to which FlK belongs (42, 43) and the strong driving force for thioester hydrolysis ($\Delta G \sim -8$ kcal/mol) (44). In this work, we show that the major mode of FlK substrate selectivity is based not on molecular recognition of fluorine but instead on exploitation of a unique chemical mechanism that is accessible only to the fluorinated substrate.

The selectivity for fluorine displayed by FlK is conferred by the lowered pK_a of the fluoracetyl-CoA α protons that allow access to an unexpected but kinetically advantageous C_α-deprotonation pathway rather than the slower pathway provided by direct reaction at the carbonyl group, as is observed for acetyl-CoA. Although C_α deprotonation itself is observed in many systems (34, 35, 45, 46), especially those involved in acyl-CoA metabolism (46), its use in initiating thioester hydrolysis of a native biological substrate is unprecedented. In this regard, the unusual reactivity of FlK allows us to explore the existence of a unique chemical species in enzyme catalysis because it strongly suggests a ketene intermediate in the FlK catalytic cycle based on similarities to related chemical model systems (38–40). Although precedence for ketene intermediates exists for enzymatic reactions with mechanism-based inhibitors or nonphysiological substrates (47–54), there is not yet any experimental evidence for their involvement in normal catalytic cycles despite their rich history in organic chemistry and the strong interest in their discovery in enzyme catalysis. For example, a ketene-based mechanism has been proposed in the catalytic cycle of glycine reductase, but it represents only one of several mechanistic possibilities that remain to be distinguished experimentally (55). FlK may therefore provide a key example of a physiological ketene intermediate derived from a native substrate in biological catalysis.

Our kinetic and biochemical data suggest that an enzyme–anhydride intermediate is formed for the nonfluorinated substrate, which would be consistent with the observation of a similar anhydride intermediate for the 4-HBT thioesterases (30, 31). Although a simpler mechanistic possibility exists for the fluorinated substrate where C_α deprotonation would occur directly on the fluoroacetyl-CoA substrate itself with concomitant formation of CoA, the burst-phase kinetics observed with [$^2H_2$]fluoroacetyl-CoA and the H76A mutant suggest that covalent catalysis is also used with the fluorinated substrate. The formation of an enzyme anhydride with the fluorinated substrate may be related to preserved evolutionary relationships with other thioesterases in the hotdog-fold superfamily but also would serve to provide a more activated leaving group to promote ketene formation.

In summary, FlK provides a unique platform to examine the evolution of substrate selectivity in a native system in which natural selection has been driven with respect to both substrates, which are estimated to be present simultaneously in the cell under saturating conditions. Although there are many examples of catalytic selectivity in enzyme superfamilies where a shared intermediate can partition between divergent downstream pathways (56, 57), FlK uses reaction partitioning to distinguish between substrates rather than to control product distribution. Indeed, the same overall transformation is catalyzed by FlK with both substrates even though two distinct reaction mechanisms occur within the same active site. Interestingly, control over reaction partitioning by the substrate is also reminiscent of the function of mechanism-based inhibitors, many of which contain fluorine themselves (58). However, these alternative substrates have been optimized by design (58) or evolution (59) to inactivate the target enzyme rather than providing a natural mechanism for exclusion of the incorrect substrate, as is observed for FlK. Taken together, FlK provides insight into the role of catalytic diversity for controlling substrate selectivity at the cellular level rather than in the evolution of new metabolic transformations.

Methods

Purification of FlK. FlK was purified as described previously (24). Protein was stored in single-use aliquots at −80 °C in 20 mM Tris·HCl (pH 7.6), 50 mM NaCl, 10% (vol/vol) glycerol.

Synthesis of Substrates. Sodium [$^2H_2$]fluoroacetate was prepared by exchange of the α protons of fluoropyruvic acid in a solution of [$^2H_2$]sulfuric acid (2.6 M) in D_2O at 120 °C under 300-W microwave irradiation for 180 min. The resultant [$^2H_2$]fluoropyruvic acid was decarboxylated to fluoroacetic acid using hydrogen peroxide. A single resonance in the ^{19}F NMR spectrum of sodium [$^2H_2$]fluoroacetate indicated the absence of monodeuterated and undeuterated sodium fluoroacetate.

Fluoroacetyl-CoA (**3**), [$^2H_2$]fluoroacetyl-CoA (**12**), and cyanoacetyl-CoA (**11**) were synthesized by activation of sodium fluoroacetate, sodium [$^2H_2$] fluoroacetate, or cyanoacetic acid to the corresponding acyl chloride using oxalyl chloride and dimethylformamide (DMF) in THF (22, 24). The crude acyl chloride was then added to a solution of CoA hydrate and triethylamine in DMF to yield the acyl-CoA. Chloroacetyl-CoA (**10**), bromoacetyl-CoA (**9**), and [$^2H_3$]acetyl-CoA (**13**) were synthesized by addition of the corresponding acyl anhydride to a solution of CoA hydrate and triethylamine in DMF (60). Reaction mixtures were quenched with water and lyophilized before purification by RP-HPLC (*SI Appendix*, Fig. S10).

3,3,3-Trifluoropropionyl-CoA (**14**) was synthesized by adding the acyl chloride to a stirred solution of CoA trilithium salt and triethylamine in water. After a 1-min reaction time, the reaction mixture was purified by RP-HPLC (*SI Appendix*, Fig. S10).

Steady-State Kinetic Experiments. Steady-state kinetic experiments were performed in triplicate as described previously (24). Enzymatic reactions were initiated by addition of FlK (5 nM–10 μM). Taft plots were constructed by plotting log k_{uncat} or log k_{cat} versus the Taft polar substituent constant σ* for the α substituent of each acyl-CoA tested (26, 61). Error bars shown on the plot for uncatalyzed hydrolysis represent the SE for three measurements of the pseudo-first-order rate constants. Error bars shown on the plot for FlK-catalyzed hydrolysis are derived from the Michaelis-Menten fits of triplicate data sets.

Pre-Steady-State Kinetic Experiments. FlK (50–150 μM) was mixed with substrate (fluoroacetyl-CoA, 500 μM; acetyl-CoA, 6,000 μM) using a KinTek Chemical Quench Flow Model RQF-3. The reaction was stopped at various times by mixing with 50% (vol/vol) TFA to achieve 17% (vol/vol) final concentration. Quenched samples were analyzed by HPLC on an Agilent Eclipse XDB-C18 column (3.5 μm, 3.0 × 150 mm) using a linear gradient from 50 mM sodium phosphate, 0.1% TFA (pH 4.5) to methanol over 15 min at 0.6 mL/min with detection of the CoA absorbance at 260 nm.

Kinetic Isotope Effect Experiments. Kinetic isotope effects were measured by direct comparison of the kinetic constants for α-deuterated and undeuterated substrates. Acetyl-CoA and [$^2H_3$]acetyl-CoA were purified by HPLC. Fluoroacetyl-CoA and [$^2H_2$]fluoroacetyl-CoA were purified three times by HPLC before use. Steady-state kinetic experiments were performed by mixing equal volumes of FlK (fluoroacetyl-CoA, 120 nM; acetyl-CoA, 20 μM) and deuterated or undeuterated substrate (fluoroacetyl-CoA, 10–200 μM; acetyl-CoA, 500–6,000 μM) using a KinTek Chemical Quench Flow Model RQF-3. The reactions were quenched and analyzed by HPLC as described for pre-steady-state kinetic experiments. Rates were determined by linear fitting of a plot of CoA formed versus time using 12–15 data points for each substrate concentration. Error bars shown for individual rates are derived from linear fitting. Kinetic isotope effects were determined by calculating the ratios k_H/k_D and $^DV/K$. Errors for the individual parameters were propagated to calculate the error for the kinetic isotope effect.

ACKNOWLEDGMENTS. We thank the Marletta Laboratory for use of their rapid chemical quench instrument and Lori Kohlstaedt (University of

California, Berkeley Vincent J. Coates Proteomics Facility) for FIK mass spectrometry analysis. The College of Chemistry NMR Facility (University of California, Berkeley) is supported in part by National Institutes of Health (NIH) Grants 1S10RR023679-01 and S10 RR16634-01. A.M.W. also acknowledges the support of NIH National Research Service Award Training Grant 1 T32 GMO66698 and a National Science Foundation Graduate Research Fellowship. This work was funded by generous support from University of California, Berkeley and NIH New Innovator Award 1 DP2 OD008696.

1. Albery WJ, Knowles JR (1976) Evolution of enzyme function and the development of catalytic efficiency. *Biochemistry* 15(25):5631–5640.
2. Page MI, Jencks WP (1971) Entropic contributions to rate accelerations in enzymic and intramolecular reactions and the chelate effect. *Proc Natl Acad Sci USA* 68(8): 1678–1683.
3. Voet JG, Abeles RH (1970) The mechanism of action of sucrose phosphorylase. Isolation and properties of a β-linked covalent glucose-enzyme complex. *J Biol Chem* 245 (5):1020–1031.
4. Kokesh FC, Westheimer FH (1971) A reporter group at the active site of acetoacetate decarboxylase. II. Ionization constant of the amino group. *J Am Chem Soc* 93(26): 7270–7274.
5. Zalatan JG, Herschlag D (2009) The far reaches of enzymology. *Nat Chem Biol* 5(8): 516–520.
6. O'Brien PJ, Herschlag D (1999) Catalytic promiscuity and the evolution of new enzymatic activities. *Chem Biol* 6(4):R91–R105.
7. Lee J, et al. (2008) Surface sites for engineering allosteric control in proteins. *Science* 322(5900):438–442.
8. Bridgham JT, Ortlund EA, Thornton JW (2009) An epistatic ratchet constrains the direction of glucocorticoid receptor evolution. *Nature* 461(7263):515–519.
9. Reynolds KA, McLaughlin RN, Ranganathan R (2011) Hot spots for allosteric regulation on protein surfaces. *Cell* 147(7):1564–1575.
10. Fischer E (1894) Einfluss der Configuration auf die Wirkung der Enzyme. *Chem Ber* 27 (3):2985–2993.
11. Koshland DE (1958) Application of a theory of enzyme specificity to protein synthesis. *Proc Natl Acad Sci USA* 44(2):98–104.
12. Boehr DD, Nussinov R, Wright PE (2009) The role of dynamic conformational ensembles in biomolecular recognition. *Nat Chem Biol* 5(11):789–796.
13. Sanada M, et al. (1986) Biosynthesis of fluorothreonine and fluoroacetic acid by the thienamycin producer, *Streptomyces cattleya*. *J Antibiot (Tokyo)* 39(2): 259–265.
14. O'Hagan D, Schaffrath C, Cobb SL, Hamilton JT, Murphy CD (2002) Biochemistry: Biosynthesis of an organofluorine molecule. *Nature* 416(6878):279.
15. Müller K, Faeh C, Diederich F (2007) Fluorine in pharmaceuticals: Looking beyond intuition. *Science* 317(5846):1881–1886.
16. Biffinger JC, Kim HW, DiMagno SG (2004) The polar hydrophobicity of fluorinated compounds. *ChemBioChem* 5(5):622–627.
17. Furuya T, Kamlet AS, Ritter T (2011) Catalysis for fluorination and trifluoromethylation. *Nature* 473(7348):470–477.
18. Gribble GW (2003) *Natural Production of Organohalogen Compounds: The Handbook of Environmental Chemistry*, ed Gribble GW (Springer, Berlin), Vol 3, pp 1–15.
19. O'Hagan D, Harper D (1999) Fluorine-containing natural products. *J Fluor Chem* 100 (1–2):127–133.
20. Clarke DD (1991) Fluoroacetate and fluorocitrate: Mechanism of action. *Neurochem Res* 16(9):1055–1058.
21. Lauble H, Kennedy MC, Emptage MH, Beinert H, Stout CD (1996) The reaction of fluorocitrate with aconitase and the crystal structure of the enzyme-inhibitor complex. *Proc Natl Acad Sci USA* 93(24):13699–13703.
22. Huang F, et al. (2006) The gene cluster for fluorometabolite biosynthesis in *Streptomyces cattleya*: A thioesterase confers resistance to fluoroacetyl-coenzyme A. *Chem Biol* 13(5):475–484.
23. Dias MV, et al. (2010) Structural basis for the activity and substrate specificity of fluoroacetyl-CoA thioesterase FIK. *J Biol Chem* 285(29):22495–22504.
24. Weeks AM, Coyle SM, Jinek M, Doudna JA, Chang MC (2010) Structural and biochemical studies of a fluoroacetyl-CoA-specific thioesterase reveal a molecular basis for fluorine selectivity. *Biochemistry* 49(43):9269–9279.
25. Shimazu M, Vetcher L, Galazzo JL, Licari P, Santi DV (2004) A sensitive and robust method for quantification of intracellular short-chain coenzyme A esters. *Anal Biochem* 328(1):51–59.
26. Taft RW, Jr. (1952) Polar and steric substituent constants for aliphatic and *o*-benzoate groups from rates of esterification and hydrolysis of esters. *J Am Chem Soc* 74(12): 3120–3128.
27. Johnson KA (1992) Transient-state kinetic analysis of enzyme reaction pathways. *The Enzymes*, ed Sigman DS (Academic, San Diego), Vol 20, pp 1–61.
28. Purich DL (2002) Covalent enzyme-substrate compounds: Detection and catalytic competence. *Methods Enzymol* 354:1–27.
29. Hartley BS, Kilby BA (1954) The reaction of *p*-nitrophenyl esters with chymotrypsin and insulin. *Biochem J* 56(2):288–297.
30. Zhuang Z, et al. (2012) Investigation of the catalytic mechanism of the hotdog-fold enzyme superfamily *Pseudomonas* sp. strain CBS3 4-hydroxybenzoyl-CoA thioesterase. *Biochemistry* 51(3):786–794.
31. Song F, et al. (2012) The catalytic mechanism of the hotdog-fold enzyme superfamily 4-hydroxybenzoyl-CoA thioesterase from *Arthrobacter* sp. strain SU. *Biochemistry* 51 (35):7000–7016.
32. Wong BJ, Gerlt JA (2003) Divergent function in the crotonase superfamily: An anhydride intermediate in the reaction catalyzed by 3-hydroxyisobutyryl-CoA hydrolase. *J Am Chem Soc* 125(40):12076–12077.
33. Hisano T, et al. (2003) Crystal structure of the (*R*)-specific enoyl-CoA hydratase from *Aeromonas caviae* involved in polyhydroxyalkanoate biosynthesis. *J Biol Chem* 278(1): 617–624.
34. Bahnson BJ, Anderson VE (1989) Isotope effects on the crotonase reaction. *Biochemistry* 28(10):4173–4181.
35. Palmer DR, Hubbard BK, Gerlt JA (1998) Evolution of enzymatic activities in the enolase superfamily: Partitioning of reactive intermediates by (*D*)-glucarate dehydratase from *Pseudomonas putida*. *Biochemistry* 37(41):14350–14357.
36. Lehrmann G, Quinn D, Cordes EH (1980) Kinetic α-deuterium isotope effects for acylation of chymotrypsin by 4-methoxyphenyl formate and for deacylation of formylchymotrypsin. *J Am Chem Soc* 102(7):2491–2492.
37. Stubbe J, Abeles RH (1977) Biotin carboxylations—Concerted or not concerted? That is the question!. *J Biol Chem* 252(23):8338–8340.
38. Holmquist B, Bruice TC (1969) The carbanion (E1cB) mechanism of ester hydrolysis. I. Hydrolysis of malonate esters. *J Am Chem Soc* 91:2993–3002.
39. Holmquist B, Bruice TC (1969) The carbanion mechanism of ester hydrolysis. II. *o*-Nitrophenyl α-cyano- and α-dimethylsulfonioacetate esters. *J Am Chem Soc* 91:3003–3009.
40. Pratt RF (1970) The carbanion mechanism (E1cB) of ester hydrolysis. III. Some structure-reactivity studies and the ketene intermediate. *J Am Chem Soc* 92:5956–5964.
41. Bruice TC, Hegarty AF, Felton SM, Donzel A, Kundu NG (1970) Aminolysis of esters. IX. The nature of the transition states in aminolysis of phenyl acetates. *J Am Chem Soc* 92:1370–1378.
42. Zhuang Z, et al. (2008) Divergence of function in the hot dog fold enzyme superfamily: The bacterial thioesterase YciA. *Biochemistry* 47(9):2789–2796.
43. Kunishima N, et al. (2005) A novel induced-fit reaction mechanism of asymmetric hot dog thioesterase PAAI. *J Mol Biol* 352(1):212–228.
44. Burton K (1955) The free energy change associated with the hydrolysis of the thiol ester bond of acetyl coenzyme A. *Biochem J* 59(1):44–46.
45. Miziorko HM, Lane MD (1977) 3-Hydroxy-3-methylgutaryl-CoA synthase. Participation of acetyl-S-enzyme and enzyme-S-hydroxymethylgutaryl-SCoA intermediates in the reaction. *J Biol Chem* 252(4):1414–1420.
46. Thompson S, et al. (1989) Mechanistic studies on β-ketoacyl thiolase from *Zoogloea ramigera*: Identification of the active-site nucleophile as Cys89, its mutation to Ser89, and kinetic and thermodynamic characterization of wild-type and mutant enzymes. *Biochemistry* 28(14):5735–5742.
47. Maycock AL, Suva RH, Abeles RH (1975) Letter: Novel inactivators of plasma amine oxidase. *J Am Chem Soc* 97(19):5613–5614.
48. Westkaemper RB, Abeles RH (1983) Novel inactivators of serine proteases based on 6-chloro-2-pyrone. *Biochemistry* 22(13):3256–3264.
49. Ortiz de Montellano PR, Komives EA (1985) Branchpoint for heme alkylation and metabolite formation in the oxidation of arylacetylenes by cytochrome P-450. *J Biol Chem* 260(6):3330–3336.
50. Blankenship JN, et al. (1991) Mechanism-based inactivation of a bacterial phosphotriesterase by an alkynyl phosphate ester. *J Am Chem Soc* 113:8560–8561.
51. Wang R, Thorpe C (1991) The reductive half-reaction in acyl-CoA oxidase from *Candida tropicalis*: Interaction with acyl-CoA analogues and an unusual thioesterase activity. *Arch Biochem Biophys* 286(2):504–510.
52. Thornburg LD, Stubbe J (1993) Mechanism-based inactivation of thymine hydroxylase, an α-ketoglutarate-dependent dioxygenase, by 5-ethynyluracil. *Biochemistry* 32 (50):14034–14042.
53. Poelarends GJ, Serrano H, Johnson WH, Jr., Whitman CP (2005) Inactivation of malonate semialdehyde decarboxylase by 3-halopropiolates: Evidence for hydratase activity. *Biochemistry* 44(26):9375–9381.
54. Gilch S, Vogel M, Lorenz MW, Meyer O, Schmidt I (2009) Interaction of the mechanism-based inactivator acetylene with ammonia monooxygenase of *Nitrosomonas europaea*. *Microbiology* 155(Pt 1):279–284.
55. Andreesen JR (2004) Glycine reductase mechanism. *Curr Opin Chem Biol* 8(5):454–461.
56. Babbitt PC, et al. (1996) The enolase superfamily: A general strategy for enzyme-catalyzed abstraction of the α-protons of carboxylic acids. *Biochemistry* 35(51): 16489–16501.
57. Eliot AC, Kirsch JF (2004) Pyridoxal phosphate enzymes: Mechanistic, structural, and evolutionary considerations. *Annu Rev Biochem* 73:383–415.
58. Berkowitz DB, Karukurichi KR, de la Salud-Bea R, Nelson DL, McCune CD (2008) Use of fluorinated functionality in enzyme inhibitor development: Mechanistic and analytical advantages. *J Fluor Chem* 129(9):731–742.
59. Groll M, Huber R, Potts BC (2006) Crystal structures of Salinosporamide A (NPI-0052) and B (NPI-0047) in complex with the 20S proteasome reveal important consequences of β-lactone ring opening and a mechanism for irreversible binding. *J Am Chem Soc* 128(15):5136–5141.
60. Yu M, de Carvalho LP, Sun G, Blanchard JS (2006) Activity-based substrate profiling for Gcn5-related *N*-acetyltransferases: The use of chloroacetyl-coenzyme A to identify protein substrates. *J Am Chem Soc* 128(48):15356–15357.
61. Hansch C, Leo A (1979) *Substituent Constants for Correlation Analysis in Chemistry and Biology* (Wiley, New York).